

## Observation of a Microscopic Cascaded Contribution to the Fifth-Order Nonlinear Susceptibility

Ksenia Dolgaleva,\* Heedeuk Shin, and Robert W. Boyd

*The Institute of Optics, University of Rochester, Rochester, New York 14627, USA*

(Received 3 May 2009; published 9 September 2009)

Typically, low-order nonlinearities are much stronger than high-order nonlinearities. In this Letter, we demonstrate a procedure by which strong high-order nonlinearities can be synthesized out of low-order nonlinearities. Our procedure involves the use of the previously largely overlooked process of microscopic cascading, which results from local-field effects. We have performed an experiment that allows us to distinguish the influence of microscopic cascading from the more-well-known process of macroscopic cascading, and we find conditions under which microscopic cascading can be the dominant effect. The ability to create a large high-order nonlinear response could prove useful for applications in quantum-information science that require the detection of the simultaneous presence of  $N$  entangled photons.

DOI: 10.1103/PhysRevLett.103.113902

PACS numbers: 42.65.An, 32.80.Wr

Nonlinear optical interactions hold great promise for many applications in optical technology and quantum-information science. The efficient excitation of nonlinear optical processes requires the use of materials with a strong nonlinear response. One means of obtaining a large value of a high-order nonlinear susceptibility is by making use of a cascaded nonlinear optical interaction, which entails using a sequence of low-order interactions to mimic a high-order response. Because lower-order nonlinearities are typically much stronger than higher-order nonlinearities, cascaded lower-order processes can be much more efficient than direct higher-order processes. It is useful to distinguish macroscopic cascading from microscopic cascading. Macroscopic cascading occurs as a result of propagation effects [1]. A classic example is that the intensity-dependent index of refraction, a  $\chi^{(3)}$  process, can be mimicked by a two-step sequence of second-harmonic generation [ $\chi^{(2)}(2\omega; \omega, \omega)$ ] followed by difference-frequency generation [ $\chi^{(2)}(\omega; 2\omega, -\omega)$ ]. Microscopic cascading is more subtle as it entails higher-order effects induced at the atomic level by means of local-field effects [2,3].

Earlier work has shown that local-field effects can enhance the linear [4] and nonlinear optical response for both homogeneous [5] and composite [6] optical materials. In a collection of three-level atoms, local-field effects can lead to inversionless gain and the enhancement of the absorptionless refractive index by more than 2 orders of magnitude [7]. In our recent publication [8], we showed how local-field effects [9] can act as a mechanism that leads to a cascaded microscopic nonlinear response. In particular, we considered nonlinear effects in a centrosymmetric medium, and we showed explicitly how the lowest-order hyperpolarizability can lead to a contribution to the fifth-order susceptibility  $\chi^{(5)}$  [8]. In this Letter, we report an experiment that verifies the existence of this microscopic cascaded contribution to  $\chi^{(5)}$ .

Bedeaux and Bloembergen first demonstrated that local-field effects can lead to microscopic cascaded contribu-

tions of the second-order hyperpolarizability  $\gamma_{\text{at}}^{(2)}$  to the third-order susceptibility  $\chi^{(3)}$  [2]. All follow-up studies conducted thus far (e.g., [3]) have concentrated on treating the local cascaded contribution of  $\gamma_{\text{at}}^{(2)}$  to third-order nonlinear effects.

In contrast, in our recent theoretical article [8], we treated the local-field-corrected fifth-order nonlinear susceptibility using two independent theoretical approaches. The first approach was based on the Maxwell-Bloch equations for a collection of two-level atoms [10], while the second approach was a more general treatment of local-field effects, based on Bloembergen's prescription [11]. Both approaches resulted in identical expressions for the local-field-corrected linear and nonlinear susceptibilities. It is convenient to represent these results in the form of the equations

$$\chi_{\text{LFC}}^{(1)} = N\gamma_{\text{at}}^{(1)}L, \quad (1a)$$

$$\chi_{\text{LFC}}^{(3)} = N\gamma_{\text{at}}^{(3)}|L|^2L^2, \quad (1b)$$

$$\chi_{\text{LFC}}^{(5)} = \chi_{\text{dir}}^{(5)} + \chi_{\text{micro}}^{(5)}, \quad (1c)$$

where we have written the fifth-order response as the sum of the two contributions

$$\chi_{\text{dir}}^{(5)} = N\gamma_{\text{at}}^{(5)}|L|^4L^2, \quad (2a)$$

$$\chi_{\text{micro}}^{(5)} = \frac{24\pi}{10}N^2(\gamma_{\text{at}}^{(3)})^2|L|^4L^3 + \frac{12\pi}{10}N^2|\gamma_{\text{at}}^{(3)}|^2|L|^6L. \quad (2b)$$

Here,  $\chi_{\text{LFC}}^{(i)}$  is the local-field corrected susceptibility of order  $i$ ,  $\gamma_{\text{at}}^{(i)}$  is the microscopic linear polarizability,  $\gamma_{\text{at}}^{(i)}$ ,  $i > 1$  is the microscopic hyperpolarizability of order  $i$ ,  $N$  is the molecular or atomic density, and  $L$  is the local-field correction factor [9]. The first contribution to the local-field-corrected fifth-order susceptibility,  $\chi_{\text{dir}}^{(5)}$  of Eq. (2a), is a direct contribution from the fifth-order microscopic hyperpolarizability. The second contribution,  $\chi_{\text{micro}}^{(5)}$  of Eq. (2b), coming from the third-order microscopic hyperpolarizability, indicates the presence of microscopic cas-

cading in  $\chi_{\text{LFC}}^{(5)}$ . This microscopic cascaded contribution to  $\chi_{\text{LFC}}^{(5)}$  is *purely* a manifestation of local-field effects. Based on the predictions of Eq. (2b), it should be possible to use microscopic cascading to induce a large cross section for three-photon absorption (which is proportional to the imaginary part of  $\chi^{(5)}$ ) by making use of a material with a large value of  $\gamma_{\text{at}}^{(3)}$ . The ability to excite three-photon absorption efficiently could have important implications to nonlinear microscopy and to quantum imaging. Such considerations motivated us to undertake a proof-of-principle experiment designed to demonstrate this microscopic cascaded contribution to  $\chi^{(5)}$ .

Our experiment is based on a degenerate multi-wave mixing (DMWM) scheme [12] (see Fig. 1) that allows one to separate the effects of different orders of nonlinearity. Two beams of equal intensity at 532 nm from a frequency-doubled Nd:YAG laser producing 35-ps pulses were sent into a 2-mm quartz cell containing a mixture of carbon disulfide ( $\text{CS}_2$ ) and fullerene  $\text{C}_{60}$ . Self-diffraction phenomena (see the photograph in Fig. 1) were observed. The first-order diffracted beam occurs as a consequence of  $\chi^{(3)}$ , whereas the second-order beam results from  $\chi^{(5)}$ .

It is clear from Eqs. (2) that  $\chi_{\text{dir}}^{(5)}$  is proportional to  $N$ , whereas  $\chi_{\text{micro}}^{(5)}$  is proportional to  $N^2$ . Hence, in order to experimentally separate the two contributions to the fifth-order susceptibility, we measured  $\chi^{(5)}$  as a function of the molecular density  $N_{\text{C}_{60}}$  of  $\text{C}_{60}$  in  $\text{CS}_2$ . For calibration reasons, we also measured the dependence for  $\chi^{(3)}$ . In order to correct the nonlinear signals for the absorption present in the medium, we measured the linear absorption coefficient  $\alpha$  and multiplied our nonlinear signal intensities by the factor  $\{\alpha l \exp(\alpha l/2)/[1 - \exp(-\alpha l)]\}^{2n}$ , where  $l$  is the length of the nonlinear medium and  $2n + 1$  is the order of the nonlinearity. We also performed an open-aperture Z-scan measurement [13] to account for nonlinear absorption. After extracting the values of the normalized transmission  $T_{\text{norm}}$  from the Z-scan measurements, we divided our nonlinear intensities by  $(T_{\text{norm}})^{2n+1}$ . The third- and fifth-order nonlinear signal intensities, corrected for the linear and nonlinear absorptions and plotted on a logarithmic scale as functions of the incident beam intensity, displayed slopes of 3 and 5, respectively.

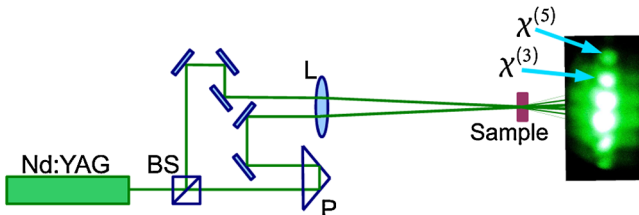


FIG. 1 (color online). Experimental setup. Nd:YAG—laser source, BS—beam splitter, P—prism, L—focusing lens,  $\chi^{(3)}$  and  $\chi^{(5)}$  denote the signals associated with these nonlinear processes.

The DMWM experiment yields the absolute values of the nonlinear susceptibilities. In order to extract these values from the measured intensities of the diffracted beams, we used the expression [12]

$$I_s = |\chi_{\text{meas}}^{(2n+1)}|^2 I_p^{2n+1} \left(\frac{8\pi}{n_0 c}\right)^{2n} \left(\frac{2\pi\omega l}{n_0 c}\right)^2 |F(\theta)|^2, \quad (3)$$

relating the measured intensity  $I_s$  of the nonlinear signal to the corresponding nonlinear susceptibility  $|\chi_{\text{meas}}^{(2n+1)}|$ . Here,  $I_p$  is the intensity of either incident beam,  $c$  is the speed of light *in vacuo*,  $n_0$  is the refractive index of the medium,  $\theta$  is a half-angle between the interacting beams in a DMWM configuration, and  $F(\theta)$  is the phase mismatch term normalized such that  $|F(0)| = 1$ .  $F(\theta)$  takes different forms for different orders of nonlinearities. For our range of molecular number densities  $N$ ,  $F(\theta)$  is a purely geometrical factor not depending on  $N$ . Substituting the measured intensity of the nonlinear signal for a mixture of  $\text{CS}_2$  and  $\text{C}_{60}$  into Eq. (3) and taking the ratio of the resulting equation to Eq. (3) with the measured intensity and known value  $\chi^{(3)} = 2.2 \times 10^{-12}$  esu [10] for pure  $\text{CS}_2$ , we find the unknown nonlinear susceptibilities.

In Fig. 2, we present the measured values of  $|\chi^{(3)}|$  and  $|\chi_{\text{eff}}^{(5)} F(\theta)|$  as functions of the molar concentration  $N_{\text{C}_{60}}$  of  $\text{C}_{60}$ . In this Letter, we do not attempt to correct the values of  $\chi_{\text{eff}}^{(5)}$  for the phase mismatch, as we cannot precisely determine the value of  $F(\theta)$  because this factor depends extremely sensitively on the alignment of our experimental setup. We instead plot the product  $|\chi_{\text{eff}}^{(5)} F(\theta)|$ , as we can extract its values directly from our data using Eq. (3). We were able to extract pure values of  $|\chi^{(3)}|$  because of the cancellation of the phase mismatch term  $F(\theta)$  upon taking the ratios of Eq. (3) for  $|\chi^{(3)}|$  signals of the mixtures of  $\text{CS}_2$  and  $\text{C}_{60}$  and pure  $\text{CS}_2$ .

$\text{CS}_2$  and  $\text{C}_{60}$  have nonlinear responses of opposite sign, which is why both the third- and fifth-order nonlinear susceptibilities in Fig. 2 decrease with the increase of  $N_{\text{C}_{60}}$ . It is clear from the graphs that  $|\chi^{(3)}|$  depends linearly on  $N_{\text{C}_{60}}$ , whereas  $|\chi_{\text{eff}}^{(5)}|$  has a quadratic dependence due to cascading. However, the *total measured* fifth-order suscep-

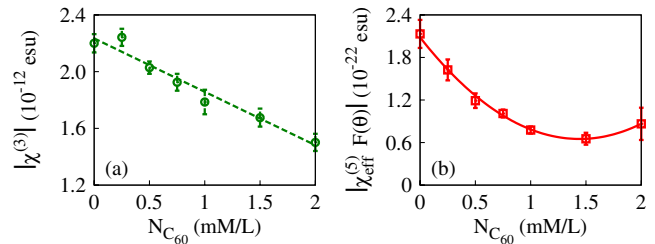


FIG. 2 (color online). Typical experimental data for (a) third-order and (b) fifth-order nonlinear susceptibilities as functions of  $N_{\text{C}_{60}}$ . The lines represent a least-square fit with a function (a) linear and (b) quadratic with respect to  $N_{\text{C}_{60}}$ .

tibility also includes the macroscopic (propagational) cascaded contribution  $|\chi_{\text{macro}}^{(5)}|$ ,

$$|\chi_{\text{eff}}^{(5)}| = |\chi_{\text{LFC}}^{(5)} + \chi_{\text{macro}}^{(5)}| = |\chi_{\text{dir}}^{(5)} + \chi_{\text{micro}}^{(5)} + \chi_{\text{macro}}^{(5)}|. \quad (4)$$

Both microscopic and macroscopic cascaded effects have a quadratic dependence on the atomic density [2], and we thus need to separate the influence of these two contributions.

To determine how to isolate the microscopic cascaded contribution, we solved the driven wave equation [10] for the direct and microscopic cascaded contributions to  $|\chi_{\text{eff}}^{(5)}|$ , and, separately, for the macroscopic-cascaded contribution. The direct and microscopic cascaded contributions to  $|\chi_{\text{eff}}^{(5)}|$  have the same dependence on phase mismatch, as they both are intrinsic properties of the nonlinear response on the molecular scale. However, the phase mismatch for  $\chi_{\text{macro}}^{(5)}$  is different from that for  $\chi_{\text{dir}}^{(5)}$  and  $\chi_{\text{micro}}^{(5)}$ . In Fig. 3, we plot the calculated efficiencies of the direct and microscopic cascaded contributions (solid line) and the macroscopic cascaded contribution (dashed line) as functions of the half-angle  $\theta$  between the interacting beams, normalized to unity at  $\theta = 0$ . The graphs show positions of the minima and maxima of the efficiencies. It is important to note that the efficiency of the macroscopic cascaded process decreases much more rapidly than that of the direct and microscopic cascaded contributions with an increase of the half-angle  $\theta$  between the interacting beams. Thus, by measuring the third- and fifth-order nonlinear signals for different values of  $\theta$ , it is possible to discriminate among the different contributions to  $|\chi_{\text{eff}}^{(5)}|$ .

The macroscopic cascaded contribution to the total electric field generated by the fifth-order nonlinear process is proportional to  $|\chi^{(3)}|^2$ . Hence, we can write  $|\chi_{\text{macro}}^{(5)}F(\theta)| = C_m|\chi^{(3)}|^2$ , where  $C_m$  is some parameter independent of  $N_{\text{C}_{60}}$ . Neglecting the direct and microscopic cascaded con-

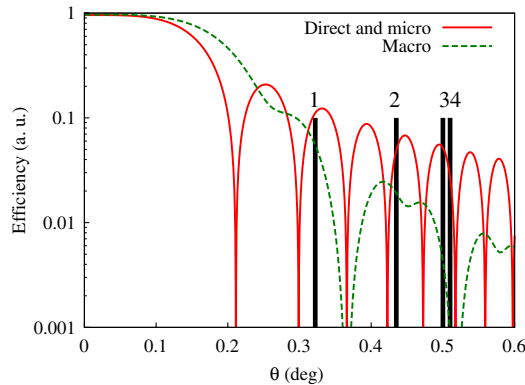


FIG. 3 (color online). Efficiency of the direct and microscopic cascaded contributions (red solid line) and the macroscopic cascaded contribution (green dashed line) as functions of the half-angle between the interacting beams. Vertical lines show the experimental cases.

tributions to the fifth-order susceptibility of pure  $\text{CS}_2$ , as their values do not change the dependence of  $|\chi_{\text{eff}}^{(5)}|$  on  $N_{\text{C}_{60}}$ , we can find  $C_m$  from the ratio  $|\chi_{\text{eff}}^{(5)}F(\theta)|/|\chi^{(3)}|^2$  at  $N_{\text{C}_{60}} = 0$ . Then, multiplying  $|\chi^{(3)}|^2$  by the value of  $C_m$ , we find  $|\chi_{\text{macro}}^{(5)}F(\theta)|$ .

We have measured the nonlinear susceptibilities at four values of the angle between the interacting beams (marked in Fig. 3 with thick vertical lines with numbers on top). The results of the measurements are shown in Fig. 4 where we plot the values of  $|\chi_{\text{eff}}^{(5)}F(\theta)|$  and  $|\chi_{\text{macro}}^{(5)}F(\theta)|$  as functions of the  $\text{C}_{60}$  concentration.

For  $\theta \approx 0.3^\circ$ , corresponding to position 1 in Fig. 3, we observed no difference between the  $|\chi_{\text{eff}}^{(5)}F(\theta)|$  and  $|\chi_{\text{macro}}^{(5)}F(\theta)|$  [see Fig. 4(a)]. This fact shows that for this experimental geometry the macroscopic cascaded contribution to  $|\chi_{\text{eff}}^{(5)}|$  is much larger than the direct and microscopic cascaded contributions. We then repeated this measurement for successively increasing values of  $\theta$ . These results are shown in parts (b) through (d) of Fig. 4. We see that as the crossing angle is increased, the difference between  $|\chi_{\text{eff}}^{(5)}F(\theta)|$  and  $|\chi_{\text{macro}}^{(5)}F(\theta)|$  becomes more and more pronounced. This difference is clearly seen in plots (c) and (d). These plots correspond to positions 3 and 4 in Fig. 3, which are very close to a minimum of the macroscopic cascading efficiency curve.

The data of Fig. 4(d) show that, under our experimental conditions, the microscopic cascaded term makes a large contribution to  $|\chi_{\text{eff}}^{(5)}|$ . This conclusion follows qualitatively from the fact that  $|\chi_{\text{eff}}^{(5)}F(\theta)|$  is significantly different from  $|\chi_{\text{macro}}^{(5)}F(\theta)|$  and shows a pronounced quadratic depen-

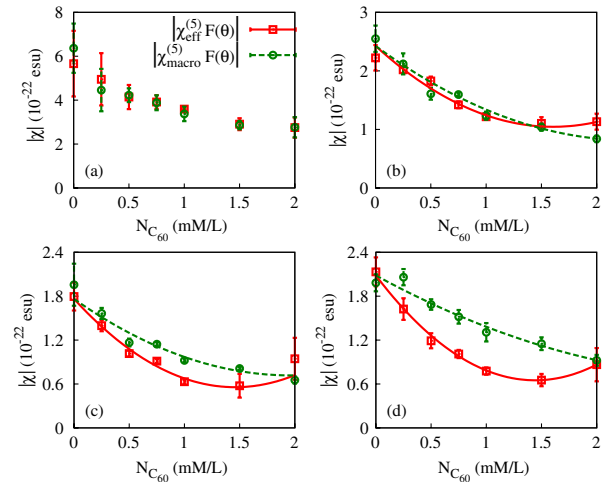


FIG. 4 (color online). Experimentally measured  $|\chi_{\text{eff}}^{(5)}F(\theta)|$  and  $|\chi_{\text{macro}}^{(5)}F(\theta)|$  as functions of  $N_{\text{C}_{60}}$ . The measurements are done at the angles between the interacting beams corresponding to (a) position 1 in Fig. 3, (b) position 2, (c) position 3, and (d) position 4. The least-square fits to the experimental data are shown with lines.

dence upon  $N$  not seen in  $|\chi_{\text{macro}}^{(5)}F(\theta)|$ . However, we are not able to extract a precise value for  $|\chi_{\text{micro}}^{(5)}|$  from our data because each of the contributions to the measured signal is a complex quantity of unknown complex phase. We have however analyzed our data in two different ways, and each analysis supports the conclusion of a large microscopic cascaded contribution to  $|\chi_{\text{eff}}^{(5)}|$ . Our first procedure is to assume that all three contributions have the same complex phase, as is the case for typical parametric nonlinearities. We then fit our data to the predictions of Eq. (4) by assuming that  $|\chi_{\text{direct}}^{(5)}|$  scales linearly with  $N_{C_{60}}$  and that  $|\chi_{\text{micro}}^{(5)}|$  and  $|\chi_{\text{macro}}^{(5)}|$  scale quadratically with  $N_{C_{60}}$ . Such an analysis leads to the conclusion that the nonlinear coefficients for  $N_{C_{60}} = 2$  mM/L are given by  $|\chi_{\text{macro}}^{(5)}F(\theta)| = 9.4 \times 10^{-23}$  esu and  $|\chi_{\text{dir}}^{(5)}F(\theta)| \approx |\chi_{\text{micro}}^{(5)}F(\theta)| \approx 1.2 \times 10^{-22}$  esu.

Our second method of analysis is to allow each of the three contributions to  $|\chi_{\text{eff}}^{(5)}|$  to have an unknown but fixed phase. For this choice of phases, we perform a fit to our data to determine the values of  $|\chi_{\text{dir}}^{(5)}|$  and  $|\chi_{\text{micro}}^{(5)}|$ . We repeat this analysis for all possible values of the relative phase at intervals of  $\pi/8$  radians. We find that for most of these relative phases the fitting procedure gives precise predictions for the fit parameters. However, in a few situations, the data can be fit by a wide range of values of the fit parameters. In the results quoted below, we include only those cases for which the uncertainty in the value of the fit parameter is less than 30%. We find that, for  $N_{C_{60}} = 2$  mM/L, the value of  $|\chi_{\text{dir}}^{(5)}|$  is in the range 2.2 to  $3.7 \times 10^{-22}$  esu and that  $|\chi_{\text{micro}}^{(5)}|$  is in the range 1.8 to  $3.7 \times 10^{-22}$  esu with  $|\chi_{\text{macro}}^{(5)}| = 9.4 \times 10^{-23}$  esu. We also find that the ratio of the parts of  $|\chi_{\text{micro}}^{(5)}|$  and  $|\chi_{\text{macro}}^{(5)}|$  that scale quadratically with the concentration  $N_{C_{60}}$  lies somewhere in the range [2.6, 5.5]. This implies that for any  $N_{C_{60}}$ , the quadratic part of  $|\chi_{\text{micro}}^{(5)}|$  is several times larger than that of  $|\chi_{\text{macro}}^{(5)}|$ .

In conclusion, we have experimentally demonstrated the existence of a local-field-induced microscopic cascaded contribution to the total fifth-order susceptibility. We have also determined the conditions under which this contribution is most significant. Even though it is sometimes easier to make use of a macroscopic cascaded process, this contribution is not always available. For example, for some experimental geometries, it is not possible to obtain a large macroscopic cascaded contribution, as is demonstrated in some of our experimental data. Also, in certain situations, such as those involving thin films, this contribution would be expected to be very weak. Moreover, absorption is always a local phenomenon, and thus macroscopic cascad-

ing makes no contribution to absorption processes, including multiphoton absorption. Thus, local-field-induced, microscopic cascaded nonlinearities are extremely important as they can potentially be made stronger than any other contribution to a high-order nonlinear process. The field of quantum-information science would benefit from the existence of efficient multiphoton absorbing materials. The results presented in this Letter may constitute an important first step in developing new nonlinear material for use in these applications.

The authors gratefully acknowledge Professor John Sipe for valuable discussions. This work was supported by a MURI grant from the US Army Research Office.

---

\*ksenia.dolgaleva@utoronto.ca; Present address: Department of Electrical and Computer Engineering, University of Toronto, 10 King's College Road, Toronto, ON M5S 3G4, Canada.

- [1] G.I. Stegeman *et al.*, Opt. Lett. **18**, 13 (1993); J.B. Khurgin, A. Obeidat, S.J. Lee, and Y.J. Ding, J. Opt. Soc. Am. B **14**, 1977 (1997); E. Yablonovitch, C. Flytzanis, and N. Bloembergen, Phys. Rev. Lett. **29**, 865 (1972).
- [2] D. Bedeaux and N. Bloembergen, Physica (Amsterdam) **69**, 57 (1973).
- [3] G.R. Meredith, Phys. Rev. B **24**, 5522 (1981); J.H. Andrews, K.L. Kowalski, and K.D. Singer, Phys. Rev. A **46**, 4172 (1992); C. Kollbeck, Phys. Rev. A **69**, 053812 (2004).
- [4] P. W. Milonni, J. Mod. Opt. **42**, 1991 (1995).
- [5] J. J. Maki, M. S. Malcuit, J. E. Sipe, and R. W. Boyd, Phys. Rev. Lett. **67**, 972 (1991).
- [6] G. L. Fischer, R. W. Boyd, R. J. Gehr, S. A. Jenekhe, J. A. Osaheni, J. E. Sipe, and L. A. Weller-Brophy, Phys. Rev. Lett. **74**, 1871 (1995); V. M. Shalaev and M. I. Stockman, Z. Phys. D **10**, 71 (1988); D. S. Chemla and D. A. B. Miller, Opt. Lett. **11**, 522 (1986).
- [7] J. P. Dowling and C. M. Bowden, Phys. Rev. Lett. **70**, 1421 (1993); A. S. Manka, J. P. Dowling, C. M. Bowden, and M. Fleischhauer, Phys. Rev. Lett. **73**, 1789 (1994); S. Singh, C. M. Bowden, and J. Rai, Opt. Commun. **135**, 93 (1997).
- [8] K. Dolgaleva, R. W. Boyd, and J. E. Sipe, Phys. Rev. A **76**, 063806 (2007).
- [9] H. A. Lorentz, *Theory of Electrons* (Teubner, Leipzig, 1916), 2nd ed.
- [10] R. W. Boyd, *Nonlinear Optics* (Academic Press, New York, 2003), 2nd ed.
- [11] N. Bloembergen, *Nonlinear Optics* (World Scientific, Singapore, 1996), 4th ed.
- [12] S. Couris, E. Koudoumas, F. Dong, and S. Leach, J. Phys. B **29**, 5033 (1996).
- [13] M. Sheik-Bahae, A. A. Said, and E. W. Van Stryland, Opt. Lett. **14**, 955 (1989).